Thin Solid Films 741 (2022) 139015

Contents lists available at ScienceDirect

Thin Solid Films

journal homepage: www.elsevier.com/locate/tsf

Enhancing thermoelectric properties of bismuth telluride and germanium telluride thin films for wearable energy harvesting

K.A. Morgan *, I. Zeimpekis, Z. Feng, D. Hewak

Optoelectronics Research Centre, Building 53, University Road, University of Southampton, UK, SO17 1BJ

ARTICLE INFO

Keywords:
Germanium telluride
Bismuth telluride
Thin film
Sputtering
Post-annealing
Flexible thermoelectric generators
Wearable technology

ABSTRACT

High performance semiconducting thin films enable the implementation of thermoelectric generators as energy harvesters for wearable applications. The optimization of material properties is critical in such applications, as restrictions introduced by the substrates on deposition temperature and active layer size, impose fundamental limitations on performance. Here we present the optimization of sputtered bismuth telluride, BiTe, and germanium telluride, GeTe, annealed at 300 °C allowing comfortable development on polyimide substrates. The crystal structure and material composition of the films, before and after annealing, were measured by X-ray diffraction and X-ray photoelectron spectroscopy to reveal the changes in the material that enhanced the performance. The power factor of the BiTe films increased post-anneal up to 2.2 μW/cmK^2, whilst the GeTe increased over 5 orders of magnitude to 7.6 μW/cmK^2. A flexible thermoelectric generator was fabricated with pairs of alternating annealed BiTe and GeTe strips, reaching 7 nW per pair of output power at a temperature difference of 20 °C. Using this micro-fabrication process of thin films, compatible to roll-to-roll technologies, the physical dimensions of the generators can be tuned to deliver the required power, for providing storage energy for on-demand devices such as periodic sensing.

1. Introduction

Flexible thermoelectric generators (f-TEGs) using thin film materials have the ability to generate uninterrupted green power from waste body heat, on flexible substrates, replacing bulky rigid energy platforms, revolutionizing the wearable and health monitoring sector [1]. They are most suited as energy harvesters for low-power devices such as sensors including temperature monitors, pressure sensors, or low-power lighting, and can be incorporated into clothing or sports equipment. However f-TEGs are held back from commercialization due to limited efficiencies of thin film materials, incompatibility with large-area high-throughput processing and a lack of module thermal and electronic management [2].

High thermoelectric performance of thin films can be achieved by lowering the thermal conductivity and electrical resistivity whilst increasing the Seebeck coefficient. Techniques such as nano-structuring or using atomically-thin films have been used to produce low thermal conductivities, although these processes are often incompatible with large-area fabrication techniques, such as roll-to-roll [3,4], commonly used for flexible electronics manufacturing. An alternate route to increasing efficiencies is to tune the power factor (PF), defined by the material's electrical conductivity and Seebeck coefficient, and the film geometry to achieve the best overall performance, compatible with flexible substrates [5]. Using the effective industrial thin film deposition technique, sputtering, the stoichiometry, crystallinity and geometry can be accurately controlled, resulting in materials with optimized PFs [6–9]. An additional step used widely throughout the electronics industry to decrease electrical resistivity is a post-deposition anneal. However, temperature limitations imposed by flexible substrates can create an additional challenge in improving the thermoelectric performance of thin films.

This work investigates the optimization of thermoelectric thin films, by annealing at a high temperature employing the robustness of a commonly used flexible substrate in the electronics industry; polyimide [10]. Unlike other polymers such as polyethylene terephthalate, commonly known as PET, polyimide can withstand 300 °C, allowing the crystallinity, stoichiometry and thermoelectric properties of thin films, to be tuned, without compromising on flexibility and bendability. Sputtering and post-deposition anneals are commonly used in micro-fabrication processing, and as such, can be used in an array of

* Corresponding author.
E-mail address: kam2g11@soton.ac.uk (K.A. Morgan).

https://doi.org/10.1016/j.tsf.2021.139015
Received 22 February 2021; Received in revised form 18 November 2021; Accepted 18 November 2021
Available online 21 November 2021

geometries and module designs, allowing easy thermal management for compatibility with a variety of end-user applications.

Germanium telluride, GeTe, a p-type thermoelectric material, has shown great promise in terms of high thermoelectric performance [6,11,12], offering similar high-performance thermoelectric properties to the commonly used n-type material, bismuth telluride, BiTe. The performance matching of both n-type and p-type materials, both of which are needed for a thermoelectric generator, is important to gain maximum efficiency at a cell level [13]. We will therefore look at both p-GeTe and n-BiTe for this work.

In this work, GeTe and BiTe thin films are directly sputtered by radio frequency (RF) magnetron co-sputtering that provides excellent control of the stoichiometry, followed by a post-deposition anneal compatible with polyimide. We investigate the effect of the anneal step on the thin films via material characterization using X-ray diffraction and energy dispersive X-ray spectroscopy. Hall-effect measurements and Seebeck measurements were conducted to investigate the annealing effects on the enhancement of power factor (1)

$$PF = \sigma S^2 \quad (1)$$

where σ is the electrical conductivity and S is the Seebeck coefficient [5]. Finally, the effects of annealing were investigated in a generator configuration, with 8 strips of BiTe and GeTe connected electrically in series and thermally in parallel.

2. Experimental

BiTe and GeTe thin films were deposited on flexible polyimide substrates (Kapton® 500HN 127 um thick) at room temperature via RF sputtering (AJA International Ltd Orion sputtering system). Before deposition, the polyimide substrates were cleaned in methanol in an ultrasonic bath for 5 min, followed by a methanol rinse and dried using a nitrogen gun. The substrates were then left overnight in a 90 °C atmospheric oven. Three commercial targets (3 inch in diameter with 99.999% purity) of bismuth, tellurium and germanium were used for co-sputtering the films. For the BiTe films, the deposition parameters used were 25 W RF for the Bi target and 30 W RF for the Te target, at a pressure of 0.13 Pa with an Ar flow of 20 sccm. For the GeTe films, the deposition parameters used were 80 W RF for the Ge target and 30 W RF for the Te target, at a pressure of 0.13 Pa with an Ar flow of 20 sccm. The BiTe films were 150 ± 5 nm thick and the GeTe films were 165 ± 5 nm, measured using a KLA-Tencor stylus profiler.

Following BiTe and GeTe deposition, Ti/Au contacts were deposited for electrical measurements using the same sputtering system. The contact deposition started with an Ar etch (2 min, 20 sccm Ar, 0.13 Pa, 30 W bias), to improve the adhesion of the contacts to the thermoelectric material but also to remove any surface oxide formed through exposure to atmosphere. 50 nm of titanium was then deposited as an adhesion layer (300 W DC, 0.27 Pa, 20 sccm Ar), followed by 150 nm of gold (300 W DC, 0.27 Pa, 20 sccm Ar). For the thermoelectric generators shadow masks laser cut from polyimide (using a Hobarts Universal PLS6MW Platform) were used to define the geometrical features. The shadow masque features are 4 cm long and 2 mm wide GeTe/BiTe strips, with 2 mm spacing between. The distance between the inner edge of the electrical contacts is 3.6 cm in length and therefore this is the effective length of the GeTe/BiTe strips. The final deposition stage was a 40 nm SiO_2 capping layer over the thin films and generators, using a SiO_2 target, with 150 W RF, 20 sccm Ar at 0.27 Pa. SiO_2 is used as a capping layer to prevent exposure of the films to atmosphere, limiting oxidation.

The anneals of the thin films and generators were performed in the sputtering system chamber, under vacuum, with a silicon wafer placed over the films to ensure the flexible substrates had a uniform and repeatable heat transfer with the chuck. The anneals were performed in 20 sccm Ar, 0.13 Pa and for 1 hour at 300 °C. The samples were left in the chamber until the system returned to room temperature to avoid oxidation when exposed to atmosphere.

The thin films were characterized in terms of crystallinity and chemical composition. The crystallinity of the films was measured by X-ray diffraction (XRD) in grazing incident (θi=1°) on a Rigaku SmartLab X-ray diffractometer with 9 kW (45 kV, 200 mA) Cu-Kα source. X-ray photoelectron spectroscopy (XPS) data was obtained using a Thermo Scientific™ Theta Probe System with Al- Kα radiation (photon energy = 1486.6 eV). After the samples were loaded, the tool reached a base pressure of 2.4e-7 Pa. Ar gas was differentially pumped in for charge neutralisation through a flood gun and etching through an ion gun. This resulted in a working pressure of 2e-4 Pa. To etch through the SiO_2 capping layer, we used the ion gun at 3 kV and 1 uA and raster scanned a 2 mm x 2 mm area for 80 s. For the analysis of the results, we used adventitious carbon at 284.8 eV and the measurements were shift corrected based on that. Peak fitting was performed using Thermo Scientific™ Avantage software, using the Al Scof library for the sensitivity factors. To fit the core levels a Shirley background was chosen in all cases. The shape of the peaks used was a Lorentzian/Gaussian mix allowed to fit but fixed between doublets. Nominal peak area ratios were used for doublets. Spin-orbit splits were advised by the software library. The stoichiometry of the BiTe and GeTe thin films were obtained from the etch step where the Si2p peak has reduced to noise level, indicating the capping layer was fully etched, ensuring the XPS is measuring the thin film below. Electrical conductivities were extracted using a Nanometrics HL5550 LN2 Hall system. The Seebeck coefficient of the films were measured using an in-house Seebeck coefficient setup as described in [6], with a B1500A Keysight Semiconductor Analyser used to measure output voltage and current. In this setup, the temperature gradient is created by using Peltier modules to generate the hot and cold surfaces, a common technique used in literature, simulating the hot Peltier as the human skin, and cold Peltier as the surrounding air [14]. In real-life applications, thermal design can enhance the temperature gradient, for example by integrating an f-TEG into a jacket leading to higher temperatures inside, whilst also reducing the thermal transport between the inside and outside of the jacket.

3. Results and discussion

3.1. Material characterization of thin films

Fig. 1 shows the XPS spectra of Bi, Ge and Te for the four thin films on polyimide. The atomic% of the four thin films were extracted from fitted XPS spectra and shown in Table 1. For the as-deposited BiTe film, bismuth is bound to tellurium in the ratio of 1:1, and a small amount of bismuth is bound to oxygen at a low percentage (< 4 at%), as demonstrated by the additional shoulder $Bi4f_{7/2}$ peak seen at 158.7 eV in Fig. 1 (a). The annealed BiTe film has a larger $Bi4f_{7/2}$ shoulder peak at a higher energy of 161.3 eV seen in Fig. 1(c), attributed to a larger oxygen content bound to bismuth (10 at%), with a bismuth to tellurium ratio of 1:1.6. This higher oxygen content suggests that oxygen, perhaps from the SiO_2 capping layer intended to limit reaction with oxygen from the atmosphere, has reacted with BiTe upon anneal. The as-deposited GeTe film and the annealed GeTe film have similar oxygen content of 37 and 38 at% respectively, with the $Ge2p_{3/2}$ shoulder peak identified at 1219.0 and 1219.2 eV in Fig. 1(e) and (g), respectively. The germanium to tellurium ratio is 1:1 and 1:1.1 for as-deposited and annealed, respectively. The compositions can be written as $Bi_{2.0}Te_{2.0}O_{0.2}$, $Bi_{2.0}Te_{3.2}O_{0.6}$, and $Ge_{1.0}Te_{1.0}O_{1.2}$, $Ge_{1.0}Te_{1.1}O_{1.3}$ for as-deposited and annealed, respectively.

XRD patterns of BiTe and GeTe thin films deposited at room temperature, with and without a post-deposition anneal, were investigated, as shown in Fig. 2. A reference sample of 40 nm SiO_2/polyimide was also measured and can be seen to produce a background signal with peaks below 2θ=30°. This is similar to XRD data seen for polyimide in literature [15–17]. Both BiTe samples show similar polycrystalline patterns, with and without a post-deposition anneal. These peaks are identified as

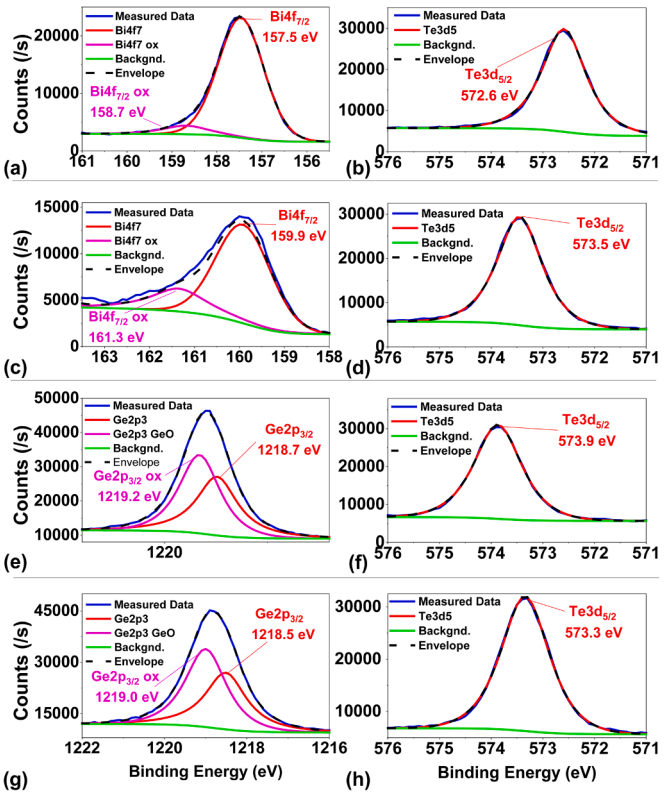

Fig. 1. XPS spectra bismuth telluride and germanium telluride films with and without a 300 °C anneal. Top row is as-deposited bismuth telluride and the second row is annealed bismuth telluride, with (a) and (c) showing the bismuth peak, and (b) and (d) the telluride peak. The third row is as-deposited germanium telluride and the last row is annealed germanium telluride, with (e) and (g) showing the germanium peak, and with (f) and (h) showing the telluride peak.

Table 1
Atomic% of BiTe and GeTe samples deposited at room temperature and annealed, extracted from XPS spectra.

	BiTe as-deposited	BiTe annealed	GeTe as-deposited	GeTe annealed
Te%	48	56	31	32
Bi%	49	35	–	–
Bi-O%	4	10	–	–
Ge%	–	–	32	30
Ge-O %	–	–	37	38

the BiTe Rhombohedral diffraction pattern, R-3m (JCPDS 002-0524). The GeTe as-deposited samples (no anneal) are lacking in defined peaks indicating highly amorphous thin films when deposited at room temperature. The annealed GeTe thin films demonstrate patterns of Rhombohedral GeTe, R-3m (JCPDS 047-1079). This indicates that the post-deposition anneal transforms amorphous as-deposited thin films into polycrystalline GeTe films. This is in agreement with rhombohedral GeTe (r-GeTe) reported in literature, described by a 6-fold coordination of Ge, with Te having three shorter and three longer bonds [18]. Cubic-GeTe (c-GeTe) is also reported in literature, seen at temperatures above 700 K, and is often thought as favourable for thermoelectric performance [18]. However, the small improvement in performance, recorded in literature as a 5% increase in figure of merit, ZT, can be seen to be outweighed by increased production costs originating from higher processing temperatures and a need for more expensive high-temperature substrates, such as ultrathin flexible glass.

Despite the lower power used for the Bi target (30 W RF) compared to the Ge target (80 W RF), with sputtering power on the individual elemental targets assisting crystallization, the BiTe films had a higher degree of crystallinity as-deposited than the GeTe films. This shows that BiTe requires less energy for crystallization than GeTe, matching the trend seen with melting temperature T_m, where BiTe's T_m is 580 °C compared to GeTe's higher T_m of 725 °C [19].

3.2. Thermoelectric properties of thin films

The post-annealing effects on the thermoelectric properties of the thin films are assessed, with room temperature Seebeck coefficient and electrical resistivities shown in Table 2 along with the subsequent power factors. The BiTe films demonstrated a negative Seebeck coefficient

Table 2
Thermoelectric properties of BiTe and GeTe thin films with and without a post-deposition anneal. The error bars represent the uncertainty of measurements for resistivity and Seebeck Coefficient.

Thin Film	Post-deposition anneal (Y/N)	Electrical Results: Electrical resistivity, ρ [mΩ-cm]	Semiconductor type	Seebeck Coefficient, S [μV/K]	Power Factor, PF [μW/cm-K^2]
BiTe	N	0.77 ± 0.05	N	−32.0 ± 0.2	1.33 ± 0.1
BiTe	Y	0.41 ± 0.05	N	−30.2 ± 0.3	2.24 ± 0.2
GeTe	N	2.77 ± 0.05×10^3	P	858.0 ± 16.0	2.66 ± 0.1 x 10^{-4}
GeTe	Y	0.61 ± 0.05	P	67.9 ± 0.8	7.58 ± 0.8

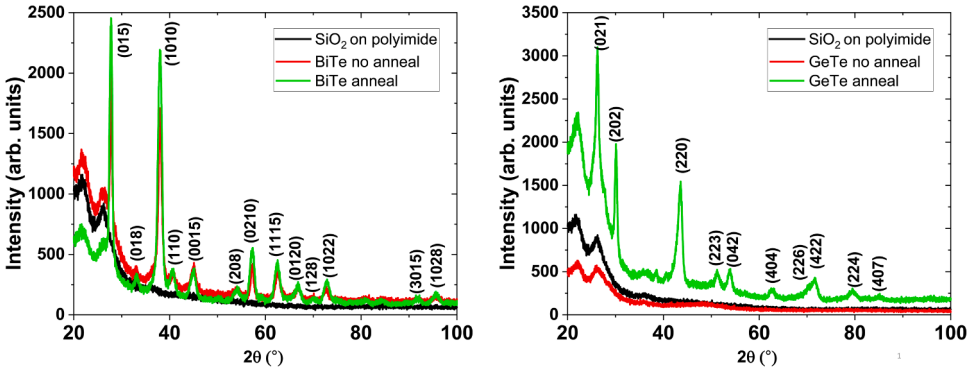

Fig. 2. XRD patterns of BiTe (left) and GeTe (right) with and without a post-deposition anneal. Reference samples of silica on polyimide are included. The labelled peaks are for BiTe (left) and GeTe (right).

indicating n-type, whilst the GeTe films demonstrated a positive Seebeck coefficient, indicating p-type behaviour. The electrical resistivity is given by

$$\rho = \frac{1}{ne\mu} \tag{2}$$

where n is the carrier concentration, e is the electron charge and μ is the carrier mobility [20]. The Seebeck coefficient of a semiconductor can be expressed as,

$$S = \frac{2k_B^2 Tm^*}{3eh^2}\left(\frac{\pi}{3n}\right)^{\frac{2}{3}}\left(\frac{3}{2}+\gamma\right) \tag{3}$$

where k_B is the Boltzmann constant, h is the reduced Plank constant, e is the electron charge, γ is the scattering factor, m^* is the effective mass and n is the carrier concentration [20].

The annealed BiTe film shows an increased conductivity when compared to the unannealed film. The stability of the Seebeck coefficient within the measurement error, combined with an unchanged crystal structure as show by the XRD results of Fig. 2, indicate no significant change in transport characteristics. The change in conductivity could more likely be attributed to an improvement in contact resistance, occurring when annealed by alloying of the contact interface.

The thermoelectric effects of GeTe thin films have the same trends as seen for BiTe, but with significantly larger changes in resistivity and Seebeck coefficients. For the GeTe thin films, an increase of four orders of magnitude in resistivity is seen when annealed. This sizable change in resistivity could be attributed to the significant change in the microstructure of the films as verified by XRD. The change from amorphous to rhombohedral GeTe results in grain growth which can lead to a significant increase in carrier mobility by facilitating current flow along large grains, therefore decreasing electrical resistivity, as demonstrated by Eq. (2) [21–23]. The GeTe thin films Seebeck coefficient significantly decreased upon annealing, dropping by an order of magnitude. This can be attributed to the growth of crystals and associated boundaries, leading to a smaller scattering factor, thus reducing the Seebeck coefficient, as seen in Eq. (3). There could also a contributing factor from an increase in carrier concertation, seen by a slightly higher Te concentration from XPS upon annealing.

When looking at the power factor, the slight reduction in Seebeck coefficient for the annealed BiTe thin films is compensated by the reduction in electrical resistivity, leading to a power factor nearly twice as large, compared to the as-deposited BiTe thin films. This shows that an anneal performed at the maximum temperature budget of the flexible substrate can be used to optimize the thermoelectric performance of BiTe films. The power factor obtained by the annealed BiTe thin films are similar to those reported for sputtered BiTe films annealed at 300C (4.0 μW/cm-K^2) and BiTe films sputtered at 250 °C (5.1 μW/cm-K^2) [6, 23], whilst the Seebeck coefficients are within the typical range from −10 uV/K up to −250 uV/K, reported for other sputtered bismuth telluride films in literature [24–26]. For the GeTe films, the four orders of magnitude decrease in electrical resistivity outweighs the decrease in Seebeck coefficient, leading to a Power Factor enhancement of four orders of magnitude. This highlights the ability to use a flexible substrate compatible anneal to optimize the thermoelectric performance of GeTe films. This power factor is within the experimental error of the GeTe thin films sputtered at 250 °C in [6].

3.3. Thermoelectric properties of generators

In the previous section, the anneal step was shown to improve the power factor of thin films. These thin films can be used in the form of a thermoelectric generator, which when connected to an external circuit, acts as an energy harvester. Two important output parameters that need to be considered for powering an external circuit are the generator output voltage and power. Whilst the power factor of the thin films is a good indicator allowing the effect of anneals on a singular material to be seen, the output performance of a generator that consists of two different materials is also dependent on material property relations (the difference in n-type and p-type performance), module geometry, heat design and connected load power requirements. The conversion efficiency of a generator is linked to the thermoelectric material properties and the geometric cross-sectional areas of the p and n-type legs. The optimum geometry is met when the ratio of the cross-sectional areas of the p-type (A_p) and n-type (A_n) is given by

$$\frac{A_n}{A_p} = \sqrt{\frac{\rho_n \kappa_p}{\rho_p \kappa_n}} \tag{4}$$

where ρ is the electrical resistivity of n and p, and κ is the thermal conductivity of n and p. Therefore, we have evaluated the thin film performance in a planar generator format, measuring the output voltage and power, with and without an anneal step. The planar design is commonly used with thin film thermoelectric generators, as it allows for easy manipulation of the geometry (via thickness and length alteration of thermocouple arms) using highly controllable thin film deposition techniques [27]. In a planar design, the heat flow direction is along the "length" of the thermoelectric strips of material, allowing for easier integration into wearables, whereby the heat gradient can be maintained due to longer lengths separating the hot and cold side.

The output performance of the two generators, with and without an anneal, is shown in Fig. 3. The output voltage and therefore Seebeck of the generator is reduced when an anneal is performed, compared to the as-deposited generator, in agreement with the trend seen for the individual thin films. The output power shows a significant increase when an anneal is performed, increasing over four orders of magnitude. Whilst an increase output voltage may seem advantageous, the limited output power, originating from the high resistivity of the unannealed thin films, leads to a significant challenge when using the films in a flexible generator as thickness restrictions will result in high resistance making load matching challenging. For ΔT=13 K, the temperature gradient typically available in wearable applications, the output voltage and power of the annealed four pair device is 3 mV and 0.2 nW [27]. The output power can be scaled up according to the needs of specific application by parallel/series arrangement of BiTe/GeTe pairs. This can also be mitigated by design optimization of the geometry of the harvester to accommodate for size restrictions.

These results show that careful material engineering in combination with component optimisation in the device and system level is paramount for applications that cannot accommodate bulky energy harvesters. Flexible thermoelectric generators have benefited from materials such as polyimide that allow for thermal tuning of the materials. The trade-off is the limited thickness of the semiconductors that

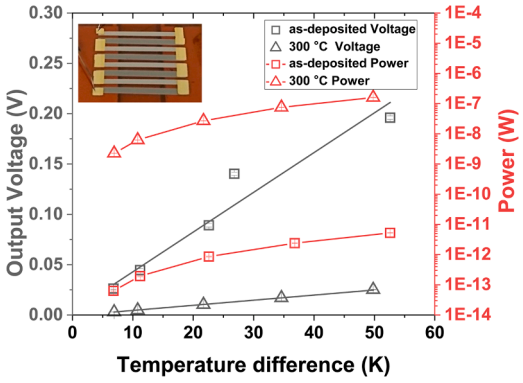

Fig. 3. Thermoelectric generator output parameters with four BiTe/GeTe p-n pairs, on polyimide, with and without an anneal. A linear fit of the voltage data signifies the Seebeck Coefficient. Inset shows photograph of the annealed device.

can withstand bending. We have found experimentally that for BiTe and GeTe this limit is close to 5 μm for moderate bending, beyond that thickness any bending results in cracking of the films. This significantly restricts the geometry tuning when compared to the bulk counterparts. Different harvester circuits have different cold start voltage and current requirements and since the thickness of the material is restricted property tailoring using annealing offers a significant advantage. For example, analog Device's LTC3108 can power up with just 20 mV and 3 mA to start charging in contrast e-peas AEM20940 requires 60 mV and 2.5 mA whereas AEM10941 requires 380 mV and 8 uA. As it can be seen there is not only a vast range of start-up power requirements but also a wide range of voltages and current requirements. This can be accommodated at the material optimisation. For example, a system that requires frequent cold start-ups at high voltages could benefit from a lower anneal temperature material. Although this might seem originally that it will affect the output power, harvester chips present much higher efficiencies at higher input voltages. The material performance parameters presented in this work can therefore be used to optimise a thermoelectric harvester system within the restricted parameter space imposed by wearable and flexible applications.

4. Conclusions

This study investigated the annealing effects on thermoelectric properties of bismuth telluride and germanium telluride films thin films, at the higher temperature budget polyimide can withstand, a commonly used flexible substrate for the electronics industry. The films were annealed at 100 °C under Ar for 1 h, and the crystallinity and stoichiometry were measured. The microstructure of the bismuth telluride films was similar with and without an anneal, exhibiting Rh-3m polycrystalline structures and a small reduction in electrical conductivity and Seebeck coefficient. Despite this Seebeck coefficient reduction, the anneal resulted in an improvement in power factor up to 2.2 μW/cm-K^2. The microstructure of the germanium telluride films changed significantly upon annealing, amorphous with no anneal and R-3m with an anneal, linking to significant changes in electrical resistivity and thus increasing the power factor from 0.3 nW/cm-K^2 to 7.6 μW/cm-K^2.

A fabrication of a BiTe and GeTe cell was demonstrated, with the annealed cell giving an output voltage of 3 mV and 0.2 nW of power at a temperature difference of 13 °C.

Data availability

All data supporting this study are openly available from the University of Southampton repository at https://doi.org/10.5258/SOTON/D1713.

CRediT author statement

K. A. Morgan contributed on the conceptualization, methodology, analysis, investigation, data curation, writing the original draft, visualization and project administration.

I. Zeimpekis contributed to the methodology, analysis, investigation and in the writing - review and editing.

Z. Feng contributed to the investigation, data curation and visualization.

D. Hewak contributed in the writing – review and editing, the supervision, resources and funding acquisition.

Declaration of Competing Interest

The authors declare that they have no known competing financial interests or personal relationships that could have appeared to influence the work reported in this paper.

Declaration of Competing Interest

The authors declare that they have no known competing financial interests or personal relationships that could have appeared to influence the work reported in this paper.

Acknowledgements

The authors acknowledge Mr Christopher Craig, Mr Ed Weatherby and Mr Glenn Topley for technical support, and Mr Mark Long and Mr Tony Gardner for making the laser cut shadow masks. This project has received funding from the European Union's Horizon 2020 research and innovation programme under grant agreement No 825143, project Smart2Go.

References

[1] Y. Du, J. Xu, B. Paul, P. Eklund, Flexible thermoelectric materials and devices, Appl. Mater. Today. 12 (2018) 366–388, https://doi.org/10.1016/j.apmt.2018.07.004.

[2] A.R.M. Siddique, S. Mahmud, B. Van Heyst, A review of the state of the science on wearable thermoelectric power generators (TEGs) and their existing challenges, Renew. Sustain. Energy Rev. 73 (2017) 730–744, https://doi.org/10.1016/j.rser.2017.01.177.

[3] K. Khan, A.K. Tareen, M. Aslam, R. Wang, Y. Zhang, A. Mahmood, Z. Ouyang, H. Zhang, Z. Guo, Recent developments in emerging two-dimensional materials and their applications, J. Mater. Chem. C. 8 (2020) 387–440, https://doi.org/10.1039/c9tc04187g.

[4] J.R. Szczech, J.M. Higgins, S. Jin, Enhancement of the thermoelectric properties in nanoscale and nanostructured materials, J. Mater. Chem. 21 (2011) 4037–4055, https://doi.org/10.1039/c0jm02755c.

[5] A. Mehdizadeh Dehkordi, M. Zebarjadi, J. He, T.M. Tritt, Thermoelectric power factor: enhancement mechanisms and strategies for higher performance thermoelectric materials, Mater. Sci. Eng. R Reports 97 (2015) 1–22, https://doi.org/10.1016/j.mser.2015.08.001.

[6] K.A. Morgan, T. Tang, I. Zeimpekis, A. Ravagli, C. Craig, J. Yao, Z. Feng, D. Yarmolich, C. Barker, H. Assender, D.W. Hewak, High-throughput physical vapour deposition flexible thermoelectric generators, Sci. Rep. 9 (2019) 1–9, https://doi.org/10.1038/s41598-019-41000-y.

[7] M. Goto, M. Sasaki, Y. Xu, T. Zhan, Y. Isoda, Y. Shinohara, Control of p-type and n-type thermoelectric properties of bismuth telluride thin films by combinatorial sputter coating technology, Appl. Surf. Sci. 407 (2017) 405–411, https://doi.org/10.1016/j.apsusc.2017.02.187.

[8] S. Shen, W. Zhu, Y. Deng, H. Zhao, Y. Peng, C. Wang, Enhancing thermoelectric properties of Sb 2 Te 3 flexible thin film through microstructure control and crystal preferential orientation engineering, Appl. Surf. Sci. 414 (2017) 197–204, https://doi.org/10.1016/j.apsusc.2017.04.074.

[9] P. Fan, Y.Z. Li, Z.H. Zheng, Q.Y. Lin, J.T. Luo, G.X. Liang, M.Q. Zhang, M.C. Chen, Thermoelectric properties optimization of Al-doped ZnO thin films prepared by reactive sputtering Zn-Al alloy target, Appl. Surf. Sci. 284 (2013) 145–149, https://doi.org/10.1016/j.apsusc.2013.07.070.

[10] A. Liu, S. Jiang, Z. Zhu, S. Zhang, D. Kang, L. Tao, Prospects and challenges in low-dimensional materials and devices for Internet of things, in: L. Tao, D. Akinwande (Eds.), Emerging 2D Materials Devices for the Internet of Things: Information, Sensing and Energy Applications, Elsevier Science, 2020, pp. 291–327, https://doi.org/10.1016/b978-0-12-818386-1.00011-4.

[11] Y. Jin, Y. Xiao, D. Wang, Z. Huang, Y. Qiu, L.D. Zhao, Realizing high thermoelectric performance in GeTe through optimizing Ge vacancies and manipulating Ge precipitates, ACS Appl. Energy Mater. 2 (2019) 7594–7601, https://doi.org/10.1021/acsaem.9b01585.

[12] J. Li, Z. Chen, X. Zhang, Y. Sun, J. Yang, Y. Pei, Electronic origin of the high thermoelectric performance of GeTe among the p-type group IV monotellurides, NPG Asia Mater 9 (2017), https://doi.org/10.1038/am.2017.8.

[13] Q. Wang, R. Quhe, Z. Guan, L. Wu, J. Bi, P. Guan, M. Lei, P. Lu, High n-type and p-type thermoelectric performance of two-dimensional SiTe at high temperature, RSC Adv. 8 (2018) 21280–21287, https://doi.org/10.1039/c8ra02270d.

[14] A. Nozariasbmarz, H. Collins, K. Dsouza, M.H. Polash, M. Hosseini, M. Hyland, J. Liu, A. Malhotra, F.M. Ortiz, F. Mohaddes, V.P. Ramesh, Y. Sargolzaeiaval, N. Snouwaert, M.C. Özturk, D. Vashaee, Review of wearable thermoelectric energy harvesting: from body temperature to electronic systems, Appl. Energy 258 (2020), 114069, https://doi.org/10.1016/j.apenergy.2019.114069.

[15] C. Wang, X. Zhao, D. Tian, D. Wang, C. Chen, H. Zhou, Synthesis and characterization of novel polyimides derived from 4,4'-bis(5-amino-2-pyridinoxy) benzophenone: effect of pyridine and ketone units in the main, Des. Monomers Polym. 20 (2017) 97–105, https://doi.org/10.1080/15685551.2016.1231036.

[16] S.S. Dong, W.Z. Shao, L. Yang, H.J. Ye, L. Zhen, Surface characterization and degradation behavior of polyimide films induced by coupling irradiation treatment, RSC Adv. 8 (2018) 28152–28160, https://doi.org/10.1039/c8ra05744c.

[17] A.A. Kareem, Thermal and electrical properties of polyimide/PANI nanofiber composites prepared via in situ polymerization, Mater. Sci. Pol. 36 (2018) 283–287, https://doi.org/10.2478/msp-2018-0047.

[18] X. Zhang, Z. Bu, S. Lin, Z. Chen, W. Li, Y. Pei, GeTe Thermoelectrics, Joule. 4 (2020) 986–1003, https://doi.org/10.1016/j.joule.2020.03.004.

[19] X. Wang, H. He, N. Wang, L. Miao, Effects of annealing temperature on thermoelectric properties of Bi 2 Te 3 films prepared by co-sputtering, Appl. Surf. Sci. 276 (2013) 539–542, https://doi.org/10.1016/j.apsusc.2013.03.130.
[20] G.J. Snyder, E.S. Toberer, Complex TE meterials, Nat. Mater. 7 (2008) 105–114.
[21] D.H. Kim, G.H. Lee, Effect of rapid thermal annealing on thermoelectric properties of bismuth telluride films grown by co-sputtering, Mater. Sci. Eng. B Solid-State Mater. Adv. Technol. 131 (2006) 106–110, https://doi.org/10.1016/j.mseb.2006.03.034.
[22] S.J. Jeon, M. Oh, H. Jeon, S. Hyun, H.J. Lee, Effects of post-annealing on thermoelectric properties of bismuth-tellurium thin films deposited by co-sputtering, Microelectron. Eng. 88 (2011) 541–544, https://doi.org/10.1016/j.mee.2010.06.036.
[23] H. Huang, W. ling Luan, S. tung Tu, Influence of annealing on thermoelectric properties of bismuth telluride films grown via radio frequency magnetron sputtering, Thin Solid Films 517 (2009) 3731–3734, https://doi.org/10.1016/j.tsf.2009.01.015.
[24] D.H. Kim, E. Byon, G.H. Lee, S. Cho, Effect of deposition temperature on the structural and thermoelectric properties of bismuth telluride thin films grown by co-sputtering, Thin Solid Films 510 (2006) 148–153, https://doi.org/10.1016/j.tsf.2005.12.306.
[25] K. Singkaselit, A. Sakulkalavek, R. Sakdanuphab, Effects of annealing temperature on the structural, mechanical and electrical properties of flexible bismuth telluride thin films prepared by high-pressure RF magnetron sputtering, Adv. Nat. Sci. Nanosci. Nanotechnol. 8 (2017), https://doi.org/10.1088/2043-6254/aa7222.
[26] S.A. Haidar, Y. Gao, Y. He, J.E. Cornett, B. Chen, N.J. Coburn, C. Glynn, M. T. Dunham, K.E. Goodson, N. Sun, Deposition and fabrication of sputtered bismuth telluride and antimony telluride for microscale thermoelectric energy harvesters, Thin Solid Films 717 (2021), 138444, https://doi.org/10.1016/j.tsf.2020.138444.
[27] N. Jaziri, A. Boughamoura, J. Müller, B. Mezghani, F. Tounsi, M. Ismail, A comprehensive review of thermoelectric generators: technologies and common applications, Energy Reports 6 (2019) 264–287, https://doi.org/10.1016/j.egyr.2019.12.011.